CINAPACT-Splines: A Family of Infinitely Smooth, Accurate and Compactly Supported Splines

Bita Akram, Usman R. Alim(✉), and Faramarz F. Samavati

Department of Computer Science, University of Calgary, Calgary AB, Canada
{bakram,ualim,samavati}@ucalgary.ca

Abstract. We introduce CINAPACT-splines, a class of C^∞, accurate and compactly supported splines. The integer translates of a CINAPACT-spline form a reconstruction space that can be tuned to achieve any order of accuracy. CINAPACT-splines resemble traditional B-splines in that higher orders of accuracy are achieved by successive convolutions with a B-spline of degree zero. Unlike B-splines however, the starting point for CINAPACT-splines is an infinitely smooth and compactly supported bump function that has been properly normalized so that it fulfills the partition of unity criterion. We use our construction to design two CINAPACT-splines, and explore their properties in the context of rendering volumetric data sampled on Cartesian grids. Our results show that CINAPACT-splines, while being infinitely smooth, are capable of providing similar reconstruction accuracy compared to some well-established filters of similar cost.

1 Introduction

Volume visualization is now a common way to explore three-dimensional images arising from modalities such as Computational Tomography (CT) or Magnetic Resonance Imaging (MRI). These images typically consist of arrays of scalar values that represent information gathered from regularly sampled volumes. The reconstruction of a continuous approximation from this discrete data is a fundamental operation in volume rendering. A careful choice of this reconstruction method can benefit the rendering process by providing a smooth, precise and efficient continuous representation of the data. As the primary goal of rendering is to provide a comprehensible image, accuracy is vital. Smoothness is beneficial for many rendering applications such as shading and feature line extraction for which higher order derivatives are required. Finally, rendering is a multi-step process dealing with large amounts of data. The cost of reconstruction therefore plays an important role in the efficiency of the visualization procedure.

In visual computing, kernel-based reconstruction methods — such as linear or cubic interpolation — are well-known. These methods place a modulated kernel at each of the sample locations to reconstruct values at arbitrary locations. The accuracy and smoothness of the reconstruction is therefore directly influenced

G. Bebis et al. (Eds.): ISVC 2015, Part I, LNCS 9474, pp. 819–829, 2015.
DOI: 10.1007/978-3-319-27857-5_73

by the kernel. Compactly supported piecewise polynomial splines are a popular choice due to their efficiency. The accuracy and support-size of these kernels are tightly knit in that more accurate reconstructions require kernels with wider support. Smoothness is achieved as a by-product, more accurate splines are usually composed of higher-degree polynomials. This has important implications for volume rendering where higher order derivatives are sometimes needed. When the reconstruction kernel does not possess sufficient smoothness, a digital derivative filter is employed to approximate the derivative at the sample locations, and then combined with the reconstruction kernel to approximate the derivative at arbitrary locations [1]. While this method ensures that the approximated derivative has the same level of smoothness as the reconstruction kernel, it adds a filtering overhead that adversely affects rendering performance.

In this paper, we introduce a novel family that consists of kernels that are explicitly constructed to be infinitely smooth (C^∞), but can be tuned to achieve any order of accuracy while maintaining compact support. We call these kernels CINAPACT-splines; they are a generalization of the recently proposed CINPACT (C^∞ and compactly supported) splines of Runions and Samavati [2] that are based on the Partition of Unity Parametrics (PUPs) framework [3]. CINPACT-splines satisfy the partition of unity criterion and therefore guarantee first-order accuracy. CINAPACT-splines improve upon the accuracy using a convolution procedure that is similar to the procedure used in the construction of uniform B-splines. Like the B-splines, CINAPACT-splines also exhibit a trade-off between higher levels of accuracy and efficiency. Unlike the B-splines however, CINAPACT splines are infinitely smooth irrespective of the order of accuracy. Despite this advantage, our tests show that CINAPACT-splines possess approximation characteristics that are comparable to some of the best known kernels. This makes them ideal candidates for applications like volume rendering.

The remainder of the paper is organized as follows. Before reviewing some important prior art (Sect. 2) that has inspired the design of CINAPACT-splines, we summarize key concepts from signal processing that are needed in our construction scheme (Sect. 1.1). The details of our construction procedure and some concrete examples that of practical significance are presented in Sect. 3. Finally, Sect. 4 presents some rendering tests that show that CINAPACT-splines, while being infinitely smooth, yield highly accurate results as compared to some well-known polynomial-spline kernels.

1.1 Preliminaries

In signal processing, interpolation is a common way to reconstruct an approximation of a function from its samples. According to Shannon's sampling theorem, a band-limited univariate function can be perfectly recovered using an ideal *sinc* kernel, if and only if the sampling rate $T < \frac{\pi}{w_{max}}$, where w_{max} is the highest frequency in the band-limited function [4].

Aliasing: As most real-world functions are not band-limited, and applying ideal reconstruction kernels is not practical owing to their infinite support, aliasing

issues occur. Pre-aliasing happens when the function is not band-limited or the sampling rate is not adequately high. Post-aliasing on the other hand, can occur when the reconstruction kernel is not ideal.

Generalized Sampling Theory: Developed by Blu and Unser [5], this theory extends Shannon's sampling theory by allowing a wider range of non-ideal kernels, ψ, while trying to minimize aliasing errors [6]. These kernels constitute an approximation space that is spanned by uniform shifts of a kernel. Approximated functions then belong to the following shift-invariant space:

$$V(\psi, T) = \left\{ \tilde{f}(x) = \sum_{n \in \mathbb{Z}} c_n \psi(x/T - n) : [c] \in l_2 \right\}. \tag{1}$$

Here, c_n is the nth component of the set of coefficients $[c]$, and the kernel $\psi \in L_2$.

Approximation Order and the Strang-Fix Conditions: The overall quality of reconstruction is affected by various factors such as the choice of the kernel ψ, and how the set of coefficients $[c]$ is determined from the available data. Approximation order is an effective tool for quantifying the quality of a reconstruction scheme. A reconstruction scheme has approximation order k if there exists a constant C such that [7]:

$$\|f - \tilde{f}\|_2 = CT^k \|f^{(k)}\|_2, \quad \text{as} \quad T \to 0. \tag{2}$$

Here, $f^{(k)}$ is the kth derivative of the function to be approximated, and $\|\cdot\|_2$ denotes the L_2 norm. If a kernel ψ provides a kth order reconstruction, it is referred to as a kth order kernel. A kth order kernel ψ satisfies the following Fourier domain conditions (*Strang-Fix conditions*) [7]:

$$\hat{\psi}(0) = 1 \quad \text{and} \quad \hat{\psi}^{(\alpha)}(\beta) = 0 \text{ for } \alpha < k \text{ and } \beta \in \left\{ 2\pi l \mid l \in \mathbb{Z} \backslash \{0\} \right\}, \tag{3}$$

where $\hat{\psi}(\cdot)$ denotes the Fourier transform of ψ. In other words, ψ is a kth order kernel if and only if its Fourier transform and the derivatives of its Fourier transform up to order k vanish at integer multiplies of 2π. The Fourier transform of the ideal kernel, i.e. the *sinc* function, is a rectangular pulse (or box function) which is completely localized; the ideal kernel therefore trivially satisfies the Strang-Fix conditions. Due to the uncertainty principle, the Fourier transform of a compactly supported kernel is not localized. The Strang-Fix conditions quantify how the transform decays to zero; the higher the approximation order, the faster the decay and the more accurate the approximation.

Partition of Unity: In order to ensure that a reconstruction scheme can approximate a given function with arbitrary accuracy, k must at least be one. Using the Poisson summation formula, it can be shown that the first approximation order ($k = 1$) implies that the integer translates of ψ form a partition of unity [5], i.e.

$$\sum_{n \in \mathbb{Z}} \psi(x - n) = 1, \quad \forall x \in \mathbb{R}. \tag{4}$$

Interpolation: Once a kth order kernel ψ has been chosen, one needs to ensure that the coefficients $[c]$ are determined in a way that respects the approximation order. In applications such as volume rendering, the function f is known through its idealized samples $[f]$ only. In this case, it is sufficient to ensure that the approximation $\tilde{f}$ interpolates the sample values, i.e. $\tilde{f}(Tn) = f_n$ [5]. As explained in Sect. 3.1, this is achieved through the application of a discrete interpolation pre-filter that is completely determined from the integer samples of ψ.

2 Related Work

Reconstruction kernels play an important role in the fields of data visualization and graphics. In the literature, a variety of kernels that satisfy different desirable properties such as simplicity, interpolation, smoothness, compact support, efficiency, and accuracy, is in use. There is usually a trade-off between different properties, and the nature of the application dictates the choice of the kernel. In this section, we look through some of the most common and useful designs of reconstruction kernels. We focus on univariate kernels with the understanding that they can be extended to higher dimensional integer grids via a simple tensor product extension. It should be noted that the design methodology behind CINAPACT splines is general and can also be applied to non-separable multivariate kernels such as radial basis functions [8] and box splines [9].

Piecewise polynomial splines are a good alternative to the ideal *sinc* function. They are built through junctions of polynomials pieced together at points called knots [10]. Uniform B-splines, introduced by Schoenberg [11], are well-known examples of this family. They have good reconstruction characteristics such as partition of unity, approximation order and compact support of $k+1$, and C^{k-1} continuity for polynomial degree k.

In 2001, Blu *et al.* introduced a family of compactly supported kernels with maximal order and minimal support (MOMS) [12]. Using their error kernel [13], they proved that the minimally-supported kernel of approximation order $k+1$ is piecewise-polynomial with degree k and support $k+1$. Uniform B-splines are a well-known member of the MOMS family and have the highest continuity among their peers [12]. Though all members of the MOMS family have maximal order for a specified support, the optimal MOMS (O-MOMS) subcategory optimizes the constant C in Eq. 2. However, these kernels have C^0 continuity and thus are not differentiable. While O-MOMS can provide us with high accuracy, we cannot neglect the importance of continuity in the quality of reconstruction [14].

Partition of Unity Parametrics (PUPs) is a flexible framework for metamodeling introduced by Runions and Samavati [3]. In this framework, any function $R(x)$ can be employed after proper normalization to satisfy partition of unity. The general form of PUPs is as follows:

$$\psi(x) = \frac{R(x)}{\sum_{j\in\mathbb{Z}} R(x-j)}, \text{ where } \sum_{j\in\mathbb{Z}} R(x-j) \neq 0. \tag{5}$$

Partition of unity also ensures a first-order approximation which, according to the Strang-Fix theory, implies a linear relationship between error reduction and sampling rate increase. Satisfying partition of unity is therefore a necessary criterion for a kernel. Runions and Samavati suggested B-spline based PUPs and employed it in the reconstruction of curves and surfaces, and also demonstrated their advantages in feature sketching and converting planar meshes into parametric surfaces [3]. In a follow-up work, they used the PUPs framework to design a new family of C^∞ and compactly supported kernels called CINPACT-splines [2]. These kernels are obtained by truncating an exponential function to preserve its smoothness while providing compact support. The resulting *bump* function is then normalized to satisfy partition of unity. Moreover, this kernel can be designed to interpolate the tangents of curves and surfaces as well as their sample points. The bump function used in the design of CINPACT-splines is defined as:

$$R(x) := \begin{cases} \exp(\frac{-kx^2}{c^2-x^2}), & x \in (-c, c), \\ 0, & \text{otherwise.} \end{cases} \tag{6}$$

The support of $R(x)$ is $2c$, and k is a continuous parameter that behaves like the polynomial degree of a B-spline if chosen correctly [2]. We therefore refer to k as the degree of the CINPACT-spline. Thus, CINPACT-splines can be considered to be a potential replacement for B-splines.

Though PUPs can be designed to serve as non-separable filters, their application in providing a framework for designing separable filters applicable to regular grids is the focus of our research. As demonstrated by some of the works described above, several properties that were believed to be strongly related, are in fact independent. For instance, Runions and Samavati have shown that smoothness and support can vary independently [2,3]. The interrelation between approximation order and level of continuity was also relaxed by the introduction of O-MOMS [12]. Drawing inspiration from these studies, the question is if we can design a filter that is infinitely smooth and has arbitrary approximation order, while preserving other beneficial properties such as compact support.

3 C^∞, Accurate and Compact Splines

CINPACT-splines provide two of the most important features for rendering applications: infinite smoothness and compact support. However, partition of unity only guarantees a first-order approximation. We need a technique to increase the approximation order while preserving infinite smoothness and compact support.

Using the Fourier convolution theorem and the Strang-Fix conditions, it can be readily shown that the convolution of two kernels having approximation orders a and b, yields a kernel with approximation order $a + b$. Hence, convolving a CINPACT-spline with the box-function (B-spline of degree zero and order one) increases its approximation order by one, and yields a *CINAPACT* spline with a minimum guaranteed order of two. Thus, we have

$$\psi^2(x) := \frac{R(x)}{\sum_{j\in\mathbb{Z}} R(x-j)} * \beta^0(x), \tag{7}$$

where $R(x)$ is the bump function introduced in Eq. 6, $\beta^0(x)$ denotes the B-spline of degree zero, and the symbol '$*$' indicates the continuous convolution operation. In order to further improve the approximation order, the initial CINPACT-spline is successively convolved with the box-function. The CINAPACT-spline with a minimum guaranteed order of L is constructed through the convolution of the normalized bump-function with the B-spline of degree $L-2$:

$$\psi^L(x) := \frac{R(x)}{\sum_{j\in\mathbb{Z}} R(x-j)} * \beta^{L-2}(x), \text{ where } L \geq 2. \tag{8}$$

Each convolution adds one unit to the support and increases the approximation order by one. Although the accuracy of CINAPACT-splines can increase arbitrarily, the cost of reconstruction increases exponentially in higher dimensions as the support size grows.

The infinite smoothness of CINPACT-splines is inherited by CINAPACT-splines through the convolution. The mth derivative of the CINAPACT spline $\psi^L(x)$ is given by

$$\psi^{L(m)}(x) = \left(\frac{R(x)}{\sum_j R(x-j)} * \beta^{L-2}(x)\right)^{(m)} = \left(\frac{R(x)}{\sum_j R(x-j)}\right)^{(m)} * \beta^{L-2}(x). \tag{9}$$

One difficulty that arises is due to the nature of the convolution integral in Eq. 8. We are currently unaware of an analytical closed form for this integral. We therefore use a quadrature method to table the values of CINAPACT splines at closely sampled locations within their support. The derivatives are also computed in a similar manner using Eq. 9. Figure 1 shows a second-order CINAPACT spline of support size four along with its first and second derivatives.

3.1 Interpolation

Similar to B-splines, the kernels within the CINAPACT-spline family are not interpolative. Recall that a kernel ψ is interpolative if and only if $\psi(x)$ vanishes at all non-zero integers. For an interpolative kernel, one can simply use the sample values $[f]$ as coefficients in Eq. 1. When a kernel is not interpolative, a discrete pre-filtering operation is necessary to ensure that the approximation $\tilde{f}(x)$ exactly reproduces the sample values. The resulting approximation (for $T = 1$) is given by

$$\tilde{f}(x) = \sum_{n\in\mathbb{Z}} c_n \psi(x-n), \text{ where } [c] = [\psi]^{-1} \otimes [f]. \tag{10}$$

Here, $[\psi]$ is a discrete filter that consists of the integer samples of ψ, i.e. $\psi_n = \psi(n)$, and $[\psi]^{-1}$ is its inverse. The symbol '$\otimes$' denotes the discrete convolution operation. In practice, for finite dimensional data, the discrete convolution in the above equation can be applied in the Fourier domain using the discrete Fourier transform which imposes periodic boundary conditions. Other types of boundary conditions can also be imposed by suitably padding the data vector $[f]$.

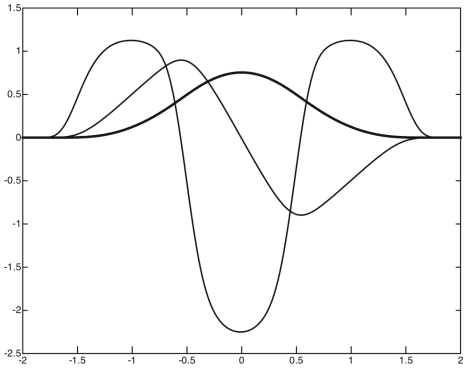

Fig. 1. The CINAPACT-spline $\psi^2(x)$ ($c = 1.5$, $k = 4$) and its first two derivatives.

3.2 Cardinal Kernel Optimization

The interpolative pre-filter and the reconstruction kernel in Eq. 10 can be combined into an interpolative *cardinal kernel* ψ_{int} so that

$$\tilde{f}(x) = \sum_{n \in \mathbb{Z}} f_n \psi_{\mathsf{int}}(x - n), \text{ where } \psi_{\mathsf{int}}(x) := \sum_{j \in \mathbb{Z}} \psi_j^{-1} \psi(x - j). \tag{11}$$

This interpolative scheme respects the overall approximation order of ψ. By inspecting the behaviour of the Fourier transform of the cardinal kernel ψ_{int}, one can also reason about the overall quality of a reconstruction scheme. Using Eq. 11, we infer that the Fourier transform of the cardinal kernel is

$$\hat{\psi}_{\mathsf{int}}(\omega) = \hat{\psi}(\omega) / \widehat{[\psi]}(\omega), \tag{12}$$

where $\widehat{[\psi]}(\omega)$ is the discrete time Fourier transform of the filter $[\psi]$. We use Eq. 12 to tune the free parameters of CINAPACT-splines as explained below. Since we are unaware of a closed form Fourier transform of the CINAPACT-splines, we use the fast Fourier transform to approximate it.

Examples: We present two concrete examples of CINAPACT-splines that can be tuned to yield cardinal spectra that closely match the spectra of the cubic B-spline and the cubic O-MOMS. In order to ensure that the kernels are comparable, we fix the support size to four using the following two procedures.

1. $\psi_k^2(x)$: We set $c = 1.5$ and $L = 2$ in Eq. 8. The resulting CINAPACT-spline has a minimum approximation order of two.
2. $\psi_k^3(x)$: We set $c = 1$ and $L = 3$ in Eq. 8. The resulting CINAPACT-spline has a minimum approximation order of three.

In the above constructions, the degree $k \in \mathbb{R}$ is a free parameter which allows us to adjust the cardinal kernels' spectra. Figure 2a and b show the cardinal spectra

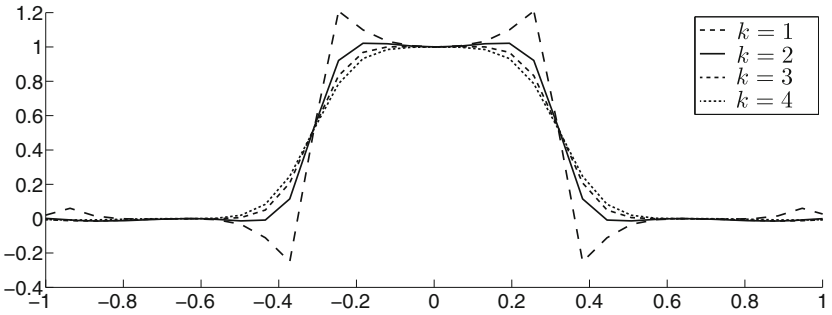

(a) Fourier spectra of the cardinal kernels of ψ_k^2.

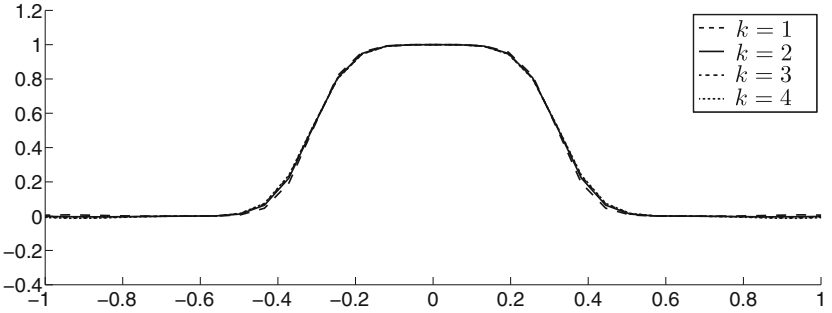

(b) Fourier spectra of the cardinal kernels of ψ_k^3.

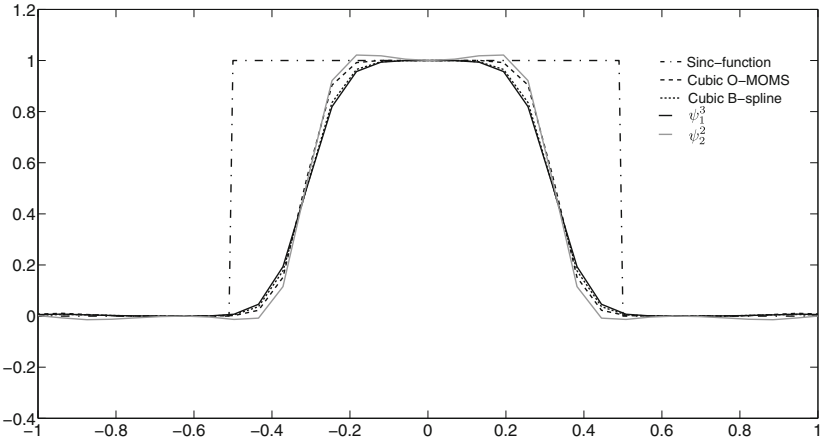

(c) Comparison of cardinal kernels in the Fourier domain.

Fig. 2. Cardinal kernels of the CINAPACT-splines ψ_2^2 and ψ_1^3 as compared to the cubic B-spline and the cubic O-MOMS.

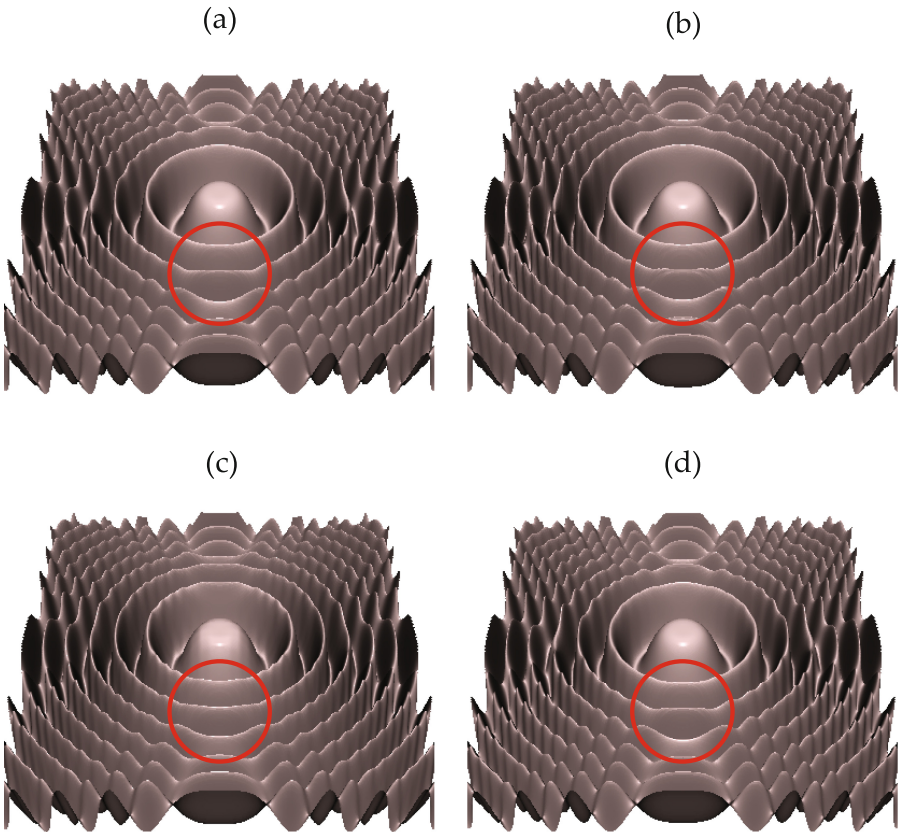

Fig. 3. Isosurface renderings of the sampled ML function using (a) cubic B-spline, (b) cubic O-MOMS, (c) ψ_2^2, and (d) ψ_1^3 (Color figure online).

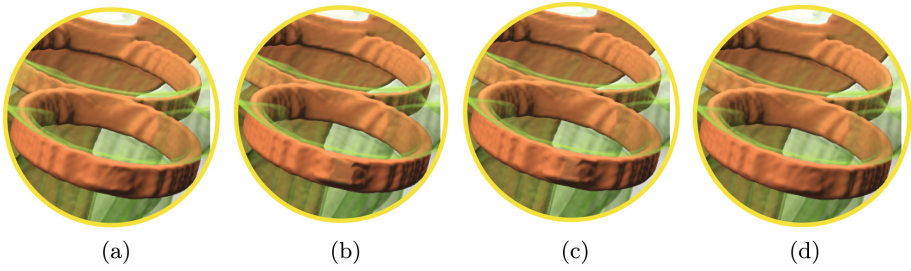

Fig. 4. Direct volume rendering results for the engine dataset using (a) cubic B-spline, (b) cubic O-MOMS, (c) ψ_2^2, and (d) ψ_1^3.

of ψ_k^2 and ψ_k^3 for various values of k. Observe that the CINAPACT-splines ψ_k^2 are much more sensitive to the degree parameter as compared to ψ_k^3 due to the lower approximation order. Among the values tested for ψ_k^2, $k = 2$ yields the best spectrum which is compared with the cardinal spectra of ψ_1^3, the cubic B-spline and the cubic O-MOMS in Fig. 2c. Observe that the cardinal spectrum of ψ_1^3 has the same behaviour as the cubic B-spline even though it has a lower guaranteed approximation order. More interestingly, the cardinal spectrum of ψ_2^2 — despite the lower approximation order — follows the O-MOMS' cardinal spectrum with some overshooting. This suggests that, with careful tuning, CINAPACT-splines can exhibit higher approximation orders than what is guaranteed; both ψ_2^2 and ψ_3^3 resemble fourth-order kernels despite their lower orders.

4 Volume Rendering Tests

We evaluated the accuracy of our proposed kernels ψ_2^2 and ψ_1^3 by rendering the 0.5 isosurface of the synthetic function suggested by Marschner and Lobb (ML) [15], and compared the results to the cubic O-MOMS and B-spline. All of these kernels have the same support, and hence the same reconstruction cost. In order to ensure that smoothness related artifacts are clear, we used the analytic first derivatives of the kernels when computing the gradient for shading. The results are shown in Fig. 3. At first glance, all the renditions look pretty similar. This is due to the fact that all four schemes behave similarly in the low-pass regime as is evident from the plot in Fig. 2c. On closer inspection, we can see subtle differences between the renditions; the cubic O-MOMS (Fig. 3b) seems to be slightly better at reconstructing the inner rings of the isosurface as compared to the cubic B-spline (Fig. 3a). However, it is also noticeably less smooth as indicated by the red circle. The rendition provided by ψ_2^2 (Fig. 3c) exhibits slightly higher undulations in the reproduction of the rings. This is owing to the overshoot of the cardinal Fourier spectrum (Fig. 2c). As predicted, ψ_1^3 (Fig. 3d) yields a rendition that is very close to the cubic B-spline. Observing the encircled regions, we see that the ψ_1^3 rendition is also slightly smoother.

When testing these four schemes in the context of direct volume rendering (DVR), we observed a similar trend. Figure 4 shows DVR images obtained from the engine CT dataset. As predicted by our Fourier analysis, the cubic B-spline and ψ_1^3 renditions (Fig. 4a and d) resemble each other, and the cubic O-MOMS are ψ_2^2 renditions (Fig. 4b and c) are very close to each other.

These results corroborate the fact that both ψ_2^2 and ψ_1^3 have higher approximation orders than anticipated, and practically behave like fourth-order B-spline kernels. It appears that the choice of the parameters c and k may be more influential than the B-spline degree (L) in determining the exact approximation order. This topic warrants further investigation.

5 Conclusion

We proposed a construction scheme that generalizes CINPACT-splines [2] to CINAPACT-splines, kernels that can be tuned to achieve any order of accu-

racy while maintaining infinite smoothness. We presented two examples of CINAPACT-splines: ψ_2^2 and ψ_1^3, that behave like fourth-order kernels. We also presented some preliminary results that suggest that, in the context of volume visualization, CINAPACT-splines may be a good alternative to B-splines due to their infinite smoothness. In future, we plan to investigate the smoothness advantage of CINAPACT-splines in more detail; potential applications include shading and feature-line extraction in a real-time volume rendering environment.

References

1. Hossain, Z., Alim, U.R., Möller, T.: Toward high quality gradient estimation on regular lattices. IEEE Trans. Visual. Comput. Graph. **17**, 426–439 (2011)
2. Runions, A., Samavati, F.: CINPACT-splines: a class of C-infinity curves with compact support. In: Boissonnat, J.-D., Cohen, A., Gibaru, O., Gout, C., Lyche, T., Mazure, M.-L., Schumaker, L.L. (eds.) Curves and Surfaces. LNCS, vol. 9213, pp. 384–398. Springer, Heidelberg (2015)
3. Runions, A., Samavati, F.F.: Partition of unity parametrics: a framework for meta-modeling. Visual Comput. **27**, 495–505 (2011)
4. Shannon, C.E.: Communication in the presence of noise. Proc. IRE **37**, 10–21 (1949)
5. Unser, M.: Sampling-50 years after shannon. Proc. IEEE **88**, 569–587 (2000)
6. Nehab, D., Hoppe, H.: A fresh look at generalized sampling. Found. Trends Comput. Graph. Vis. **8**, 1–84 (2014)
7. Strang, W., Fix, G.: An Analysis of the Finite Element Method. Prentice-Hall, Englewood Cliffs (1973). Prentice-Hall series in automatic computation
8. Buhmann, M.: Radial Basis Functions: Theory and Implementations. Cambridge University Press, New York (2003). Cambridge Monographs on Applied and Computational Mathematics
9. de Boor, C., Höllig, K., Riemenschneider, S.D.: Box splines, vol. 98. Springer, New York (1993)
10. Unser, M.: Splines: a perfect fit for signal and image processing. IEEE Signal Process. Mag. **16**, 22–38 (1999)
11. Schönberg, I.J.: Contributions to the problem of approximation of equidistant data by analytic functions. Quart. Appl. Math **4**, 45–99 (1946)
12. Blu, T., Thévenaz, P., Unser, M.: Moms: maximal-order interpolation of minimal support. IEEE Trans. Image Process. **10**, 1069–1080 (2001)
13. Blu, T., Unser, M.: Quantitative fourier analysis of approximation techniques. i. interpolators and projectors. IEEE Trans. Signal Process. **47**, 2783–2795 (1999)
14. Kindlmann, G., Whitaker, R., Tasdizen, T., Möller, T.: Curvature-based transfer functions for direct volume rendering: methods and applications. In: Visualization 2003, pp. 513–520. IEEE Computer Society Press (2003)
15. Marschner, S.R., Lobb, R.J.: An evaluation of reconstruction filters for volume rendering. In: Visualization 1994, pp. 100–107. IEEE Computer Society Press (1994)